

AD-A088 572

ARIZONA UNIV TUCSON DEPT OF CHEMISTRY

F/6 12/1

ON THE USE OF THE INVERTED ABEL INTEGRAL FOR EVALUATING SPECTRO-ETC(U)

JUL 80 J D ALGER, M B DENTON

N00014-75-C-0513

UNCLASSIFIED

TR-24

NL

1 of 1  
ALGER  
068402



END

DATE

FILED

10-80

DTIC

AD A088572

OFFICE OF NAVAL RESEARCH  
Contract N00014-75-C-0513  
Task No. NR 051-549  
Technical Report No. 24

ON THE USE OF THE INVERTED ABEL INTEGRAL  
FOR EVALUATING SPECTROSCOPIC SOURCES

by

J. D. Algeo and M. B. Denton

Prepared for Publication

in

Applied Spectroscopy

Department of Chemistry  
University of Arizona  
Tucson, Arizona 85721

July, 1980

Reproduction in whole or in part is permitted for  
any purpose of the United States Government

Approved for Public Release: Distribution Unlimited

80 8 27 030

DDC FILE COPY

REPORT DOCUMENTATION PAGE		READ INSTRUCTIONS BEFORE COMPLETING FORM
1. REPORT NUMBER 2474 TR-2.1	2. GOVT ACCESSION NO. AD-A088 572	3. RECIPIENT'S CATALOG NUMBER
4. TITLE (and Subtitle) ON THE USE OF THE INVERTED ABEL INTEGRAL FOR EVALUATING SPECTROSCOPIC SOURCES		5. TYPE OF REPORT & PERIOD COVERED INTERIM rept.
7. AUTHOR(s) J. D. ALGEO AND M. B. DENTON		8. CONTRACT OR GRANT NUMBER(s) N00014-75-C-0513
9. PERFORMING ORGANIZATION NAME AND ADDRESS Department of Chemistry University of Arizona Tucson, Arizona 85721		10. PROGRAM ELEMENT, PROJECT, TASK AREA & WORK UNIT NUMBERS NR 051-549
11. CONTROLLING OFFICE NAME AND ADDRESS Office of Naval Research Arlington, Virginia 22217		12. REPORT DATE July 1980
14. MONITORING AGENCY NAME & ADDRESS (if different from Controlling Office) 12/4/V		13. NUMBER OF PAGES 14
		15. SECURITY CLASS. (of this report) UNCLASSIFIED
		15a. DECLASSIFICATION/DOWNGRADING SCHEDULE
16. DISTRIBUTION STATEMENT (of this Report)  Approved for Public Release: Distribution Unlimited		
17. DISTRIBUTION STATEMENT (of the abstract entered in Block 20, if different from Report)		
18. SUPPLEMENTARY NOTES  Prepared for Publication in Applied Spectroscopy.		
19. KEY WORDS (Continue on reverse side if necessary and identify by block number)  Inverted Abel Integral, Cubic Spline, Three Dimentional Flame Mapping.		
20. ABSTRACT (Continue on reverse side if necessary and identify by block number) A numerical method for evaluating the inverted Abel integral employing cubic spline approximations is described along with a modification of the procedure of Cremers and Birkebak, and an extension of the Barr method. The accuracy of the computations is evaluated at several noise levels and with varying resolution of the input data. The cubic spline method is found to be useful only at very low noise levels, but capable of providing good results with small data sets. The Barr method is computationally the simplest, and is adequate when large data sets are available. For noisy data, the method of Cremers and Birkebak gave the best results.		

033860

LB

On the Use of the Inverted Abel Integral  
for Evaluating Spectroscopic Sources

by

J. D. Algeo and M. B. Denton

Department of Chemistry  
University of Arizona  
Tucson, Arizona 85721

1st		
A		

# ABSTRACT

A numerical method for evaluating the inverted Abel integral employing cubic spline approximations is described along with a modification of the procedure of Cremers and Birkebak, and an extension of the Barr method. The accuracy of the computations is evaluated at several noise levels and with varying resolution of the input data. The cubic spline method is found to be useful only at very low noise levels, but capable of providing good results with small data sets. The Barr method is computationally the simplest, and is adequate when large data sets are available. For noisy data, the method of Cremers and Birkebak gave the best results.

## BRIEF

Three methods for evaluating the inverted Abel integral are presented and their sensitivity to noise in the input data and resolution of the input data are evaluated.

## Introduction

When spectroscopic observations are made of a flame or plasma, the quantity observed generally represents an integration of the contributions to the signal by species distributed across the source in the line of observation. Detailed knowledge of the conditions at any region within the source requires the application of special techniques. Two line atomic fluorescence may be used to obtain local temperatures within flames (1, 2). The droplet injection technique developed by Heiftje and Malmstadt (3) has been shown to be useful for making spatially resolved temperature measurements (4). Two photon excitation by pulsed lasers has been proposed by Measures as an instrumental technique for obtaining spatial resolution (5). These techniques require special instrumentation and are generally applicable only to the study of temperature profiles or distributions of species possessing good atomic fluorescence characteristics. The droplet injection technique may be more general, but may not reflect the conditions obtained with nebulizer systems.

Mathematical techniques may be used to extract information about the interior from conventional side on measurements. When applied to sources of irregular shape, mathematical techniques require that measurements be made from more than one direction relative to the orientation of the source (6, 7, 8). If the source possesses a simple and regular geometry, one set of measurements will suffice. This is a common case in analytical spectroscopy, where the source often possesses circular symmetry, and may be treated by the inverted Abel integral (9, 10, 11, 12, 13, 14).

This integral may be written as:

$$i(r) = - \frac{1}{\pi} \int_r^R \frac{I'(x)}{(x^2 - r^2)^{1/2}} dx \quad (1)$$

where  $i(r)$  is the value of the variable sought as a function of the radius,  $r$ ;  $I(x)$  is the value of the observed variable as a function of the distance between the optical axis and the source axis,  $x$ ; and  $R$  is the outer radius of the source. See Figure 1.

When the inverted Abel integral is used to determine radial emission profiles, it is necessary to account for self absorption if the flame or plasma is not optically thin (15, 16, 17).

In this laboratory, we have been interested in the application of the inverted Abel integral to a variety of sources, including inductively coupled plasmas, stable analytical flames, and transient flames produced by pyrotechnic flares.

Because the transformation of a laterally observed profile into a radial profile tends to accentuate any uncertainty in the observations, it is important to evaluate the noise sensitivity of any technique used to perform the transformation. An extensive analysis of error propagation in Porter's method has been published (18), but many of the other methods have not been subjected to such scrutiny.

In this communication, we present the results of studies into the error propagation of three methods for evaluating equation (1). The methods investigated were a modification of the technique of Cremers and Birkebak (13), an extension of the method of Barr (12), and a new method, based upon Cubic Spline functions, which was developed by the authors. The methods are compared with regard to their accuracy



under varied conditions of data resolution and noise level, and recommendations are developed for which method is most suitable for a given quality of data.

### Description of the Methods

Application of the inverted Abel integral to spectroscopic data requires the construction of a suitable function,  $I(x)$ , giving the observed quantity in terms of the distance between the source axis and optical axis. A suitable function will possess the following properties: its derivative will be integrable in (1), its first derivative will have a value of zero at the source axis (i.e.,  $I'(0) = 0$ ), and it will reject noise in the observed data. The requirement that  $I'(0) = 0$  is dictated by the assumption of circular symmetry, and a failure to adhere to this constraint will generally cause a large error in the computed value of  $i(0)$ . If the function follows noise in the input data, the resulting large values of  $|I''(x)|$  will cause significant errors.

Several workers have used polynomial approximations to the unknown function,  $I(x)$  (11, 12, 13). Such functions are easily generated from the observed data, and their derivatives yield an integratable representation of Equation (1).

To allow treatment of a variety of curve shapes, the data are generally broken into several segments, each covering a portion of the range of  $x$ , and a separate polynomial is generated for each segment. These polynomials are spliced together to obtain  $I(x)$ . For the  $j^{\text{th}}$  segment, the polynomial representation of  $I(x)$  may be written:

$$I_j(x) = A_{0j} + A_{1j}x + A_{2j}x^2 + A_{3j}x^3 + \dots \quad (2)$$

with the corresponding derivative

$$I_j'(x) = A_{1j} + 2A_{2j}x + 3A_{3j}x^2 + \dots \quad (3)$$

For an approximation of this form,  $i(r)$  is obtained by a summation of Equation (1) over the appropriate segments. The following equation may be used for polynomials of fourth or lower order:

$$i(r) = \sum_j \frac{1}{\pi} \left[ A_{1j} \ln \frac{R_{j+1} + S_{j+1}}{R_j + S_j} + 2A_{2j} (S_{j+1} - S_j) + \frac{3}{2} A_{3j} \left( R_{j+1}S_{j+1} - R_jS_j + r^2 \ln \frac{R_{j+1} + S_{j+1}}{R_j + S_j} \right) + 4A_{4j} \left\{ \frac{S_{j+1}^3 - S_j^3}{3} + r^2 (S_{j+1} - S_j) \right\} \right] \quad (4)$$

where  $R_j$  is the inner radius of the  $j^{\text{th}}$  data segment, or  $r$ , whichever is greater; and  $S_j = (R_j^2 - r^2)^{1/2}$ .

#### Development of the Spline Method

Cubic Spline functions consist of a series of third order polynomials, each one covering an interval between two points. These polynomials are determined so that the composite function produced by joining them end-to-end has the following properties: the function passes through all of the points, and is therefore continuous; the first derivative is continuous; and the rate of change of the slope is minimized, that is:

$$\int f''(x)^2 dx \quad (5)$$

is minimized over the range of  $x$ .

Cubic Splines have been used for interpolating data (18,19,20); however, their properties of having a simple, continuous first derivative and a minimized rate of change of slope make them attractive as

approximations of  $I(x)$ . Reinsch (21) has addressed the problem of fitting Cubic Splines to noisy data by introducing a smoothing parameter,  $S$ , and allowing the function to pass outside of the data points, subject to the condition

$$\sum_{i=1}^N \frac{(y_i - f(x_i))^2}{(dy_i)^2} \leq S \quad (6)$$

Here  $y_i$  is the input value,  $f(x_i)$  is the value computed from the spline function, and  $dy_i$  is the weight of the  $i^{\text{th}}$  point.  $N$  is the number of data points. Reinsch suggests using the standard deviations of the data points as the weights,  $dy_i$ , and values of  $S$  in the range

$$N - \sqrt{2N} \leq S \leq N + \sqrt{2N}$$

Smoothing values well in excess of the recommended range have been explored, and, while good results were sometimes obtained, performance tended to be erratic when smoothing values larger than those recommended were used.

The spline method is implemented by first normalizing the  $x$  values to an outer radius of 1.0. Reinsch's algorithm is then applied to generate a smoothed Cubic Spline function having  $N-1$  segments. A transformation of the function is performed to give it coordinates compatible with Equation (4). Values of  $i(r)$  are computed by evaluating the first three terms of Equation (4) over each segment from  $r$  to  $R$ .

Details of the transformation are given below.

Reinsch's algorithm produces the Cubic Spline in terms of offsets,  $h_j$ , so that each segment starts at zero:

$$f_j(x - h_j) = A_{0j} + A_{1j}(x - h_j) + A_{2j}(x - h_j)^2 + A_{3j}(x - h_j)^3 \quad (7)$$

where  $h_j$  is the value of  $x$  at the inner end of the  $j^{\text{th}}$  segment.

To simplify the application of Equation (4), the spline equations are converted into functions of  $x$  as follows:

$$A^*_{0j} = A_{0j} - A_{1j}h_j + A_{2j}h_j^2 + A_{3j}h_j^3 \quad (8)$$

$$A^*_{1j} = A_{1j} - 2A_{2j}h_j + 3A_{3j}h_j^2 \quad (9)$$

$$A^*_{2j} = A_{2j} - 3A_{3j}h_j \quad (10)$$

$$A^*_{3j} = A_{3j} \quad (11)$$

This yields functions of the form:

$$f^*_j(x) = A^*_{0j} + A^*_{1j}x + A^*_{2j}x^2 + A^*_{3j}x^3, \quad (12)$$

where the  $h_j$ 's have been removed.

One further modification is necessary, since the condition  $I'(0) = 0$  is not met by the Cubic Spline function. The innermost segment's coefficients are recomputed so that  $I'(0) = 0$  while the original values at the ends of the segments are preserved, along with the continuity of the first derivative. This is accomplished by Equations (13-16):

$$A^{\#}_{00} = A^*_{00} \quad (13)$$

$$A^{\#}_{10} = 0 \quad (14)$$

$$A^{\#}_{20} = \frac{3(A^*_{11}h + A^*_{01} - A^*_{00})(N-1)}{3} - A^*_{11}(N-1) + A_{31} \quad (15)$$

$$A^{\#}_{30} = (A_{01} - A^*_{00})(N-1)^3 - A^*_{30}(N-1) \quad (16)$$

These yield the inner segment equation:

$$f^{\#}_0(x) = A^{\#}_{00} + A^{\#}_{20}x^2 + A^{\#}_{30}x^3 \quad (17)$$

Note that the value  $A_{01}$  in Equation (16) is the coefficient from Equation (7), while all other A's in the right hand sides of Equations (13-16) are from Equation (12).

The transformed polynomials  $f_0^{\#}(x)$  and  $f_1^*(x)$  through  $f_{N-1}^*(x)$  are used in Equation (4) to compute the values of  $i(r)$ .

It was found that this method produced large errors in the values of  $i(0)$  due to a sharp change in curvature in the inner segment of the spline function. The following modification was found to reduce the error, and was incorporated into the method: The point next to the center, i.e. at  $r = \frac{1}{N-1}$ , is reflected across the center to  $r = \frac{-1}{N-1}$ . The spline curve is then fitted to the  $N+1$  points from  $r = \frac{-1}{N-1}$  to  $r = 1.0$ . The segment of this spline function covering  $r = \frac{-1}{N-1}$  to  $r = 0.0$  is discarded, and the procedure is continued beginning at Equation (8). The inclusion of this extra point appears to steady the function near  $r = 0$ . Reflection of 2 or 3 points was also tried, but showed no benefit relative to reflecting 1 point.

A further attempt at reducing the error in  $i(0)$  was made by reducing the statistical weight,  $dy$ , of the points at  $r = \frac{-1}{N-1}$ ,  $r = 0$  and  $r = \frac{1}{N-1}$ . This technique did not improve the results, and was not incorporated into the method.

The Cubic Spline method, with one reflected point and equal weight on all points, will be referred to as SPLINE.

#### Extension of the Barr Method

Barr (12) developed a method of performing the Abel inversion which, while using a multisegmented polynomial approximation to  $I(x)$ , differs from other methods in that the integration is performed before

the differentiation. This reversal of the order of operations is claimed to reduce the sensitivity to noise in the input data. In addition, this method greatly reduces the amount of computation required through the use of a table of coefficients from which a sum of products is used to compute  $i(r)$ :

$$k = (N-1)r$$

$$i(r) = \frac{1}{(N-1)\pi} \sum_{n=k-2}^N \beta_{kn} I_n, \text{ for } k > 2$$

$$i(r) = \frac{1}{(N-1)\pi} \sum_{n=0}^N \beta_{kn} I_n, \text{ for } k \leq 2 \quad (18)$$

Note that  $i(r)$  may be obtained only for values of  $r$  which yield integral values of  $(N-1)r$ , and that the function  $I(x)$  need not be generated, since only the observed values,  $I_0$  through  $I_n$ , are needed.

The table of coefficients is given in Ref. (12) for  $N = 21$ . Smaller data sets are handled by the assumption that  $I(x) = 0$  for  $x \geq 1.0$ .

In order to perform a complete comparison of this method to the others studied, it was necessary to extend the table of coefficients beyond  $N = 21$ . The table has been extended to cover  $N \leq 51$  by the use of the equations presented in the appendix.

#### Modification of the Cremers and Birkebak Method

A method involving multisegmented polynomials in which the segments are overlapped to provide smoothing was developed by Cremers and Birkebak (13). The method has been implemented in this laboratory with two changes:

In order to comply with the restriction that  $I'(0) = 0$ , Cremers and Birkebak changed the form of the approximation of  $I(x)$  from Equation (2) to a fit in  $x^2$  for the innermost segment:

$$I_0\{x\} = A_{00} + A_{10}x^2 + A_{20}x^4 + A_{30}x^6 + A_{40}x^8 \quad (19)$$

To avoid changing the form of Equation (4) to allow for the high orders involved in (19), we have used Equation (2) throughout, subject to the limitation that  $A_1 = 0$  in the innermost segment. This change from the original method might also be expected to improve the results by reducing the ability of the inner segment to reproduce noise.

The amount of overlap between adjacent segments utilized in fitting the approximations to  $I(x)$ , fixed at three points in Cremers and Birkebak's work, was made variable in our modification, and is expressed in percent. Thus, a 50 % overlap specifies that one half of the points from the adjacent segments are to be used when fitting  $I(x)$ . This modification permits some variation in the amount of smoothing performed.

It was found that double precision (64 bit) math was necessary in the least squares curve fitting computation when 51 point data sets were used.

This modification of the method of Cremers and Birkebak will be referred to as C & B 3 when third order approximations to  $I(x)$  are used, and as C & B 4 when fourth order fits are employed. Except for a limited set of experiments intended for direct comparison to Ref. (9), all work with this method involved a 50 % overlap.

### Procedures

Three functions describing different shapes of  $i(r)$  vs.  $r$  were used to generate test data:

$$i(r) = 1 - 3r^2 + 2r^3, \quad (20)$$

the bell-shaped curve from Ref. (13),

$$\begin{aligned} i(r) &= 0.75 + 32r^3 \text{ over the range } 0 \leq r \leq 0.25 \text{ and} \\ i(r) &= 16/27(1 + 6r - 15r^2 + 8r^3) \text{ over the range} \\ 0.25 \leq r \leq 1.0, \end{aligned} \quad (21)$$

the off axis distribution from Ref. (13), and

$$i(r) = 0.79788e^{-8r^2}, \quad (22)$$

a Gaussian curve with  $\mu = 0$  and  $\sigma = \frac{1}{4}$ .

"True" inverted data were prepared for comparison with the various inversion methods by evaluation of these functions. "Exact" input data for the inversion calculations were prepared by integration of

$$I(x) = 2 \int_x^R \frac{i(r)r}{(r^2 - x^2)^{1/2}} dr \quad (23)$$



using (20), (21) or (22) as  $i(r)$ . These data were rounded to  $\pm 5 \times 10^{-5}$ , corresponding to a residual peak to peak noise level of approximately 0.02 %, and were assigned weights of  $5 \times 10^{-5}$  for use by SPLINE. Various amounts of noise were added from a normal distribution by a pseudorandom number generator. The noise was expressed in percent as a peak to peak value referred to the largest observation in the exact data. The standard deviation of noisy data for use by SPLINE was considered to be 1/4 of the peak to peak noise. Data sets having 11, 21, 31, 41 and 51 points each were prepared and noise was added at 0.1, 0.25, 0.5, 1, 2, 5, and 10 %. Several replicate data sets were prepared at all added noise levels.

To provide a direct comparison with the results of Cremers and Birkebak, data sets were prepared by rounding the exact values to  $\pm 0.005$ .

The accuracy of the inversion calculations was evaluated by computing the standard deviation of the errors between the computed inversion and the true inversion. This was expressed as a percentage noise in the inverted data relative to the largest value in the true inversion, again using the criterion that four standard deviations define the peak to peak noise. Two factorial design experiments were performed, and the data were subjected to Analyses of Variance.

All computations were programmed in FORTRAN and performed on a Data General NOVA computer.

### Results

The modified Cremers and Birkebak method was compared to the original using the off axis distribution of Equation (21). Both

exact data and data rounded to  $\pm 0.005$  were used, as in Ref. (13). The results are presented in Table I. The modified method performed much better than the original with 11 point data sets. Above 11 points, the original method was better when exact data were used.

The first factorial experiment used all three distributions, 11 through 41 point data sets, and from 1 through 10 percent added noise. C & B 3 was the best overall, followed by SPLINE and then BARR, with all differences significant ( $p < 0.05$ ). The three distributions produced significantly ( $p < 0.05$ ) different results, with the normal curve (Eq. 22) being the easiest to reproduce, followed by the polynomial bell (Eq. 20) and the more difficult off axis curve (Eq. 21).

Some trends are evident in the data from the first experiment (see Table II). The most striking is the failure of BARR at 11 points. Plots of the inverted output from all three curve shapes, of which Figure 2b is representative, show an overdamped appearance when compared to the output of the other methods (Figures 2a and c). Both SPLINE and BARR appear underdamped in the presence of noise when a large number of points are used, as depicted in Figures 3a and b. At the lower noise levels (1 to 2 %), BARR with 31 points worked well, as did C & B 3 with 31 or 41 points. At higher noise levels (5 to 10 %), C & B 3 was clearly superior to both SPLINE and BARR. All three distributions gave qualitatively similar results.

A second factorial experiment was undertaken to elucidate the behavior of the methods at lower noise levels. This experiment used only one distribution, Equation (21), and covered the 0.1 to 0.5 % noise range. Statistical analysis grouped SPLINE and C & B 3 together, with BARR significantly ( $p < 0.05$ ) worse, due again to the failure of BARR at 11

points. The results of this experiment are shown in Table III. All data collected on the Equation (21) distribution are summarized in Table IV and Figures 4 through 8.

These figures show that SPLINE provided the best results when the input data contained less than 0.25 % noise, and that C & B 3 was best with data containing over 0.25 % noise. BARR was very poor with 11 point data sets, becoming better as the resolution of the data increased. With small amounts of noise and 41 or 51 data points, BARR approached C & B 3, but both were less precise than SPLINE. As the noise level increased, BARR provided results intermediate to the other two methods.

As seen in Figures 4 and 7, C & B 4 was inferior to C & B 3.

### Conclusions

The choice among these methods of performing the Abel Inversion depends upon the situation at hand. If a noise level of over 0.25 is present in the data, the best results may be expected from the modified Cremers and Birkebak method, and a large number of data points should be used. Where precise data are available, the Cubic Spline method should provide the best results, if a reliable estimate of the standard deviation of the data is also available. A small set will suffice in this case. The Barr method may be chosen when simplicity of computation is important, and a large number of data points are available.

Acknowledgements

This research was partially supported by the Office of Naval Research, by an Alfred P. Sloan Foundation Research Fellowship awarded to M. B. Denton, and partially by a contract from Naval Air Systems Command.

## References

1. H. Haraguchi, B. Smith, S. Weeks, D. J. Johnson, and J. D. Winefordner, *Appl. Spectrosc.* 31, 156 (1977).
2. G. Zirzak, F. Cignoli, and S. Benecchi, *Appl. Spectrosc.* 33, 179 (1979).
3. G. M. Heiftje and H. V. Malmstadt, *Anal. Chem.* 40, 1860 (1978).
4. M. A. Fernandez and G. J. Bastiaans, *Appl. Spectrosc.* 33, 145 (1979).
5. R. M. Measures, *Appl. Spectrosc.* 32, 381 (1978).
6. H. N. Olsen, C. D. Maldonado, and G. D. Duckworth, *J. Quant. Spectrosc. Radiat Transfer* 8, 1419 (1968).
7. M. P. Freeman and S. Katz, *J. opt. Soc. Am.* 53, 1172 (1963).
8. C. D. Maldonado and H. N. Olsen, *J. Opt. Soc. Am.* 56, 1305 (1966).
9. C. D. Maldonado, A. P. Caron, and H. N. Olsen, *J. Opt. Soc. Am.* 55, 1247 (1965).
10. O. H. Nestor and H. N. Olsen, *SIAM Rev.* 2, 200 (1960).
11. K. J. Bockasten, *J. Opt. Soc. Am.* 51, 943 (1961).
12. W. L. Barr, *J. Opt. Soc. Am.* 52, 885 (1962).
13. C. J. Cremers and R. C. Birkebak, *Appl. Opt.* 5, 1057 (1966).
14. D. J. Kalnicky, R. N. Kniseley, and V. A. Fassel, *Spectrochim. Acta* 30B, 511 (1975).
15. M. P. Freeman and S. Katz, *J. Opt. Soc. Am.* 50, 826 (1960).
16. R. W. Porter, *SIAM Rev.* 6, 228 (1964).
17. A. Scheeline and J. P. Walters, *Anal. Chem.* 48, 1519 (1976).
18. D. W. Blair, *J. Quant. Spectrosc. Radiat. Transfer* 14, 325 (1974).
19. J. H. Ahlberg, E. N. Nilson, and J. L. Walsh, "The Theory of Splines and Their Applications," Academic Press, New York, 1967.

20. W. A. Halang, R. Langlais, and E. Kugler, Anal. Chem. 50, 1829 (1978).
21. C. H. Reinsch, Numer. Math. 10, 177 (1967).
22. W. L. Barr, personal communication, 1979.

Degree	Number of Points	EXACT DATA			ROUNDED DATA		
		Ref <sup>a</sup> (12)	This work, 50 % Overlap	This work, <sup>b</sup> 3 Points	Ref <sup>a</sup> (12)	This work, 50 % Overlap	This work, 3 Points
Third	11	154	1.33	9.05	153	3.87	10.15
	21	4.04	1.48	4.41	5.64	3.49	5.62
	31	1.84	1.34	1.34	3.89	2.11	2.11
	41	1.06	1.24	0.71	4.80	2.47	2.04
	51	0.73	0.66	0.54	3.69	2.52	2.05
Fourth	11	83	1.08	4.35	82	6.25	3.10
	21	1.38	1.73	2.78	4.08	3.04	2.34
	31	0.74	1.64	1.64	4.00	2.05	2.05
	41	0.53	1.53	1.01	3.94	2.98	4.33
	51	0.44	1.15	0.87	4.52	2.76	3.56

Table I. Comparison of the Modified Cremers and Birkebak method to Cremers and Birkebak's results for the curve given by Eq. 21. All data are peak to peak noise as a percent of the largest value in the true inversion.

<sup>a</sup>Values have been converted to percent noise.

<sup>b</sup>Three point overlaps were produced by the following overlap percentages: 11 points - 100 %; 21 points - 75 %; 31 points - 50 %, 41 points - 37.5 % and 51 points - 30 %. Note that the maximum overlap available with 11 point data sets is only 2 points.

Curve Shape	Method	Number of Points	INPUT NOISE, % of $I_{max}$				
			0.02	1 <sup>a</sup>	2 <sup>a</sup>	5 <sup>a</sup>	10 <sup>a</sup>
Eq. 20	SPLINE	11	0.4	2.0	4.5	12.0	13.5
		21	0.3	3.3	5.6	8.9	19.2
		31	0.4	3.0	4.9	6.9	16.2
		41	0.4	2.8	4.8	24.0	23.4
	BARR	11	6.4	6.0	6.6	11.4	17.9
		21	1.3	1.2	3.1	6.8	15.4
		31	0.6	1.9	6.0	6.3	16.2
		41	0.4	1.7	6.1	27.1	26.7
	C & B 3	11	0.7	2.2	7.5	13.3	17.7
		21	0.6	1.6	6.5	4.4	15.4
		31	0.8	1.0	2.9	3.6	12.6
		41	0.5	1.5	2.7	4.7	12.1
Eq. 21	SPLINE	11	0.7	6.4	5.1	8.8	20.0
		21	0.1	2.9	4.1	19.9	22.4
		31	0.1	3.9	6.0	13.4	21.0
		41	0.1	4.3	5.6	17.9	27.9
	BARR	11	25.6	26.8	24.9	21.8	20.4
		21	5.5	6.0	6.8	9.6	14.2
		31	2.4	2.6	3.7	10.5	22.5
		41	1.4	4.2	4.3	17.4	20.4
	C & B 3	11	1.4	4.8	3.4	7.3	15.5
		21	1.6	2.2	3.0	11.4	10.3
		31	1.6	2.2	6.0	5.1	8.9
		41	1.3	2.1	3.0	17.9	15.5
Eq. 22	SPLINE	11	0.9	1.9	5.9	8.0	8.9
		21	0.7	2.7	2.7	5.8	9.8
		31	0.6	1.6	3.2	8.3	25.3
		41	0.7	2.3	3.5	12.3	19.1
	BARR	11	17.8	18.1	18.6	15.1	20.4
		21	2.8	2.8	2.3	4.8	11.8
		31	1.0	1.2	2.1	8.5	19.4
		41	0.6	2.1	4.7	5.6	13.7
	C & B 3	11	2.8	2.8	2.7	6.5	12.9
		21	2.2	2.5	3.0	8.1	7.9
		31	2.1	2.2	2.6	3.7	6.6
		41	2.0	2.4	1.9	4.7	7.6

Table II. Noise in the computed inversion for levels of noise in the input data of up to 10%.

<sup>a</sup> Each value is the mean of 2 replicates.



Method	Number of Points	INPUT NOISE, %			
		0	0.1 <sup>a</sup>	0.25 <sup>a</sup>	0.5 <sup>a</sup>
SPLINE	11	0.66	0.89	1.52	2.59
	41	0.13	0.55	1.43	1.50
BARR	11	25.6	25.6	25.6	25.6
	41	1.37	1.36	1.54	2.14
C & B 3	11	1.40	1.42	1.57	2.09
	41	1.25	1.25	1.20	1.35

Table III. Percent noise in the computed inversion for three methods with input noise of up to 0.5 %. All data are for the off axis distribution of Eq. 21.

<sup>a</sup>Each value is the mean of 5 replicates.

		INPUT NOISE, %							
Method	Number of Points	0	0.1	0.25	0.5	1	2	5	10
SPLINE	11	0.66	0.89	1.52	2.59	6.4	5.1	8.8	20.0
	21	0.10	0.49	1.10	1.86	2.9	4.1	19.9	22.4
	31	0.14	0.79	1.17	1.92	3.9	6.0	13.4	21.0
	41	0.13	0.55	1.43	1.50	4.3	5.6	17.9	27.9
	51	0.14	0.58	1.75	2.87	5.4	5.3	17.2	24.0
BARR	11	25.57	25.60	25.61	25.64	26.8	24.9	21.8	20.4
	21	5.53	5.46	5.56	5.66	6.0	6.8	9.6	14.2
	31	2.40	2.33	2.53	2.77	2.6	3.7	10.5	22.5
	41	1.37	1.36	1.54	2.14	4.2	4.3	17.4	20.4
	51	0.88	0.93	1.46	1.94	5.3	4.1	18.5	21.8
C & B 3	11	1.40	1.42	1.57	2.09	4.8	3.4	7.3	15.5
	21	1.56	1.45	1.62	1.78	2.2	3.0	11.4	10.3
	31	1.58	1.37	1.46	1.57	2.2	6.0	5.1	8.9
	41	1.25	1.25	1.20	1.35	2.1	3.0	17.9	15.5
	51	0.90	0.89	0.94	1.05	2.2	2.3	5.5	12.0
C & B 4	11	1.46	1.70	1.95	2.76	5.1	4.9	18.3	36.8
	41	2.82	2.88	3.04	2.87	3.4	4.3	13.8	22.2

Table IV. Summary of data collected for the distribution given by Eq. 21.

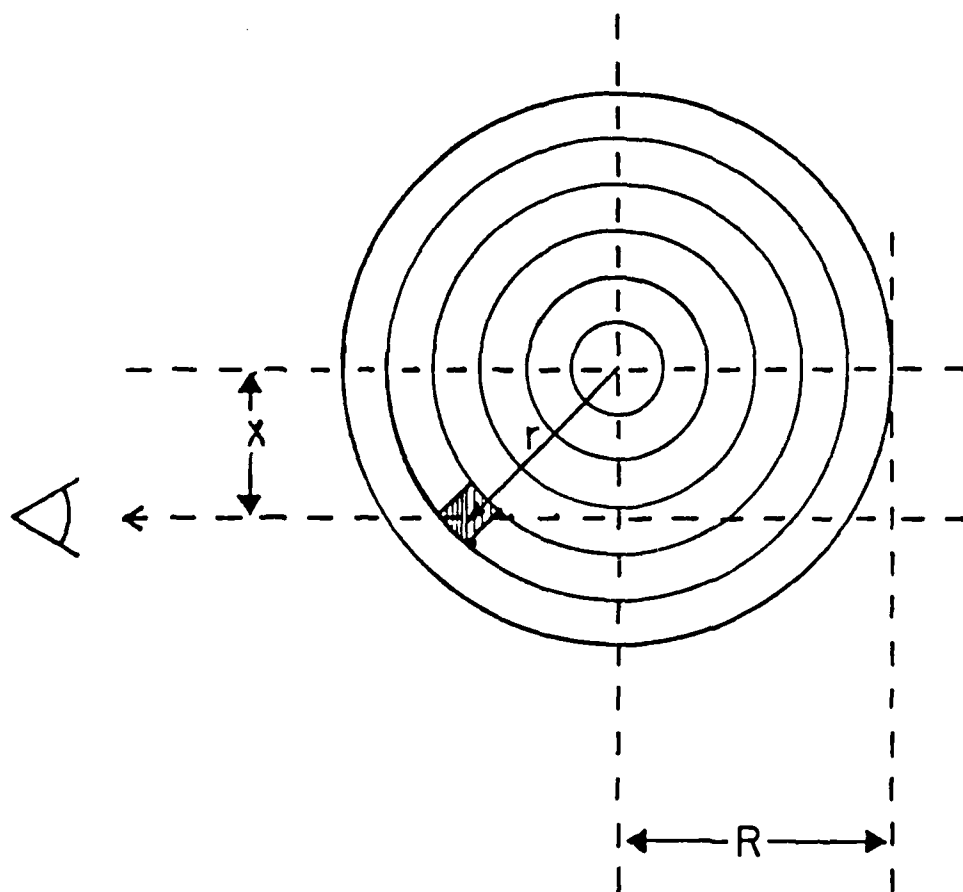


Figure 1. Top view of the experiment, showing the relationship of  $x$ ,  $r$ , and  $R$ .

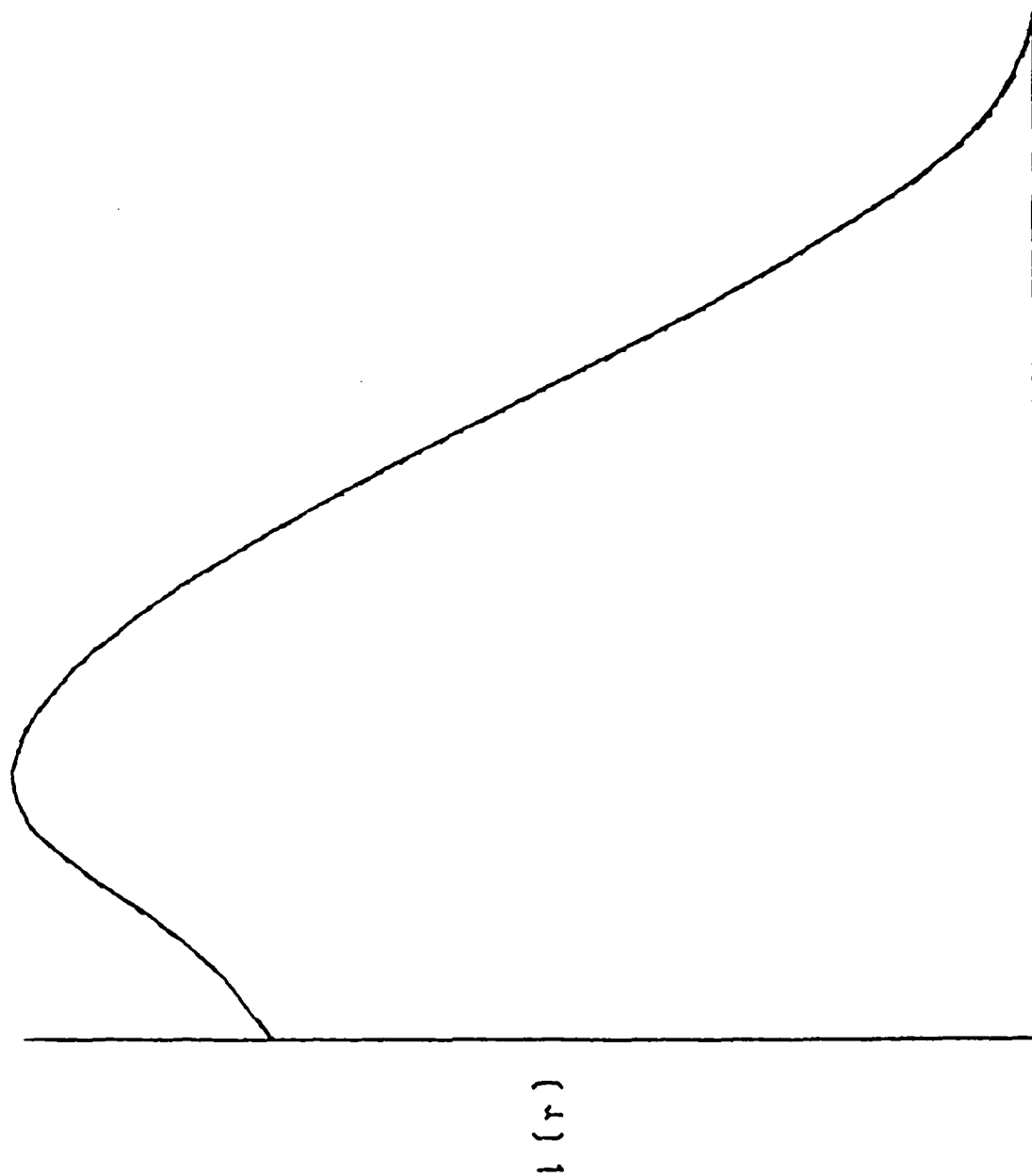
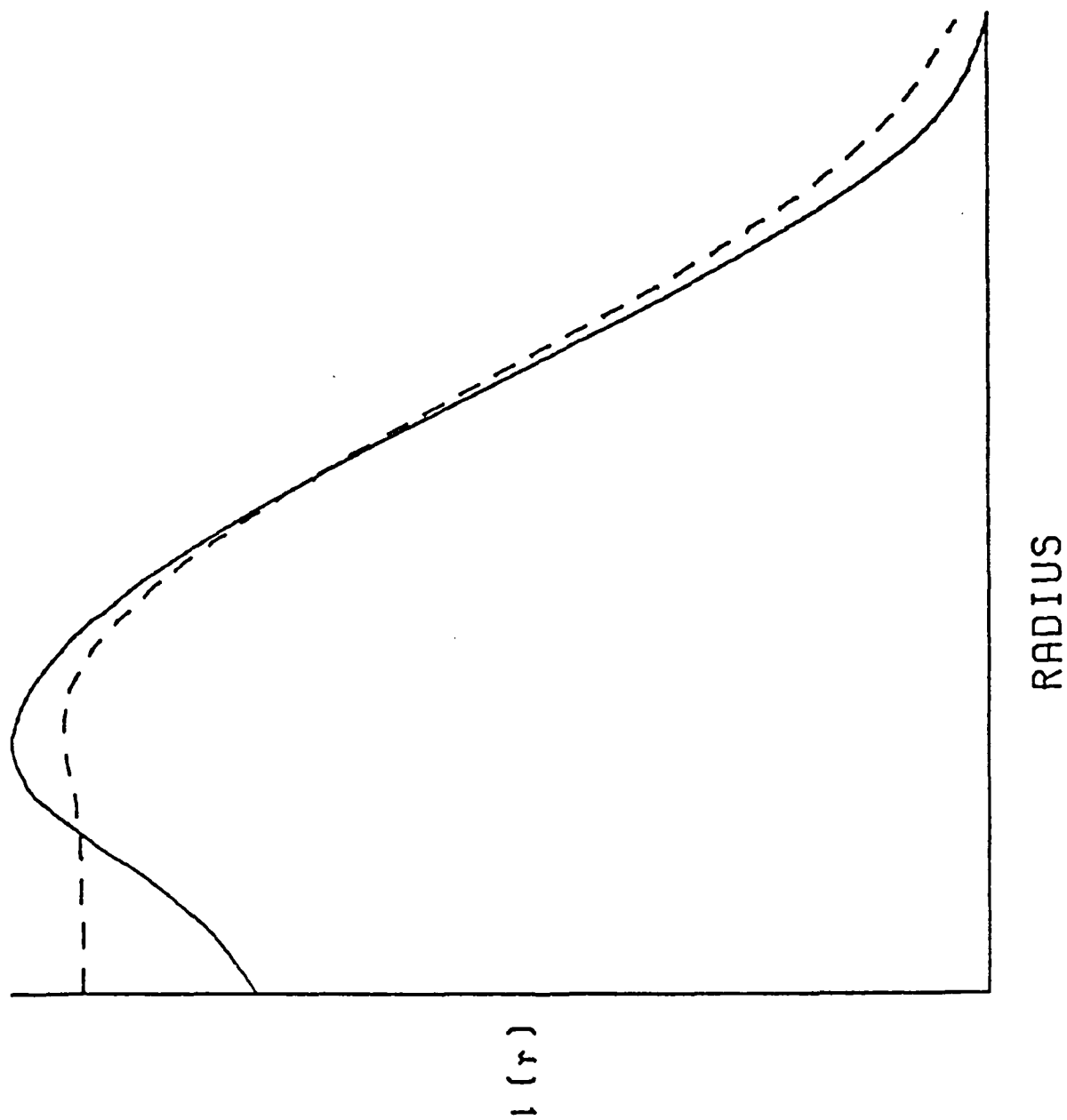
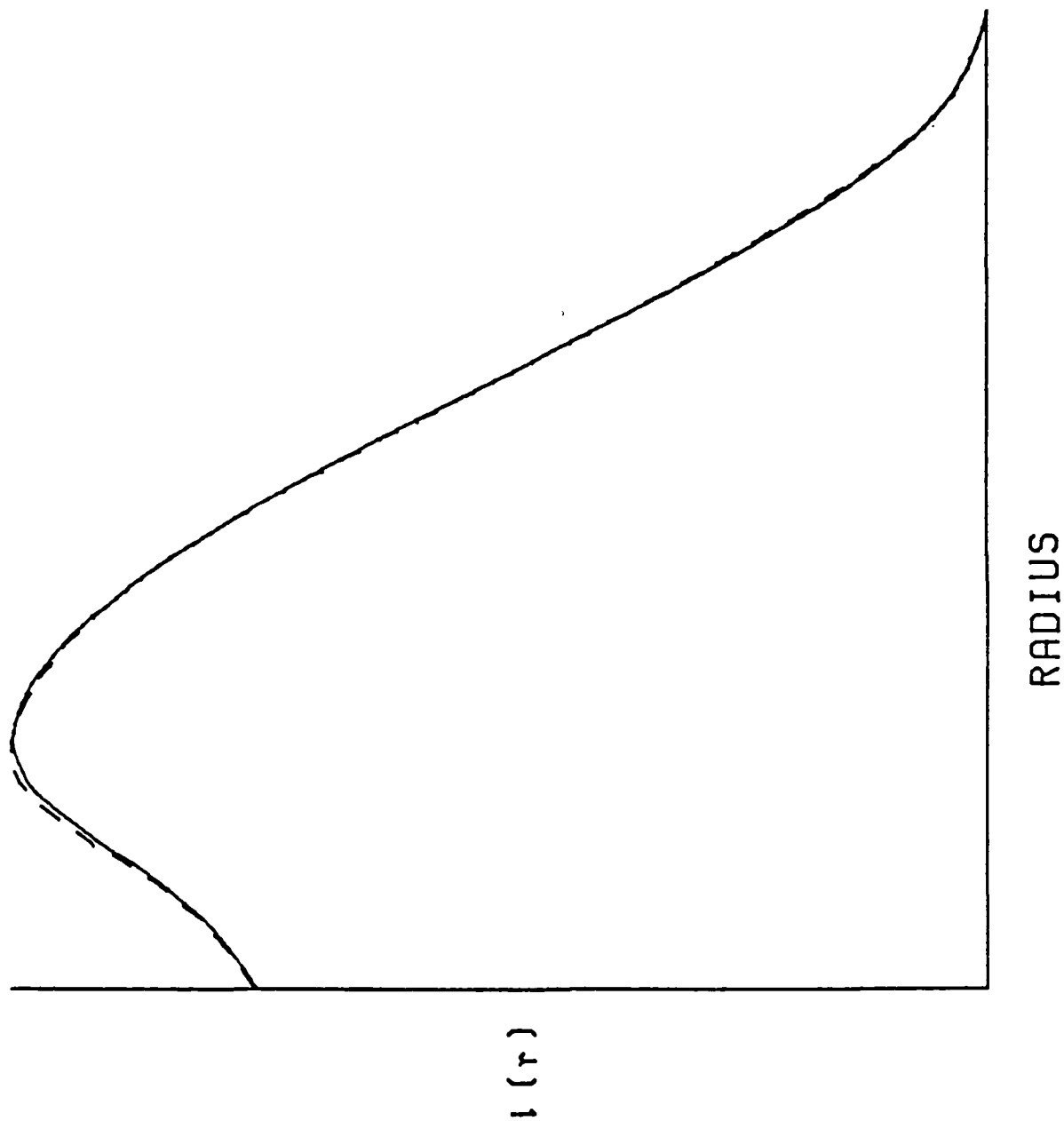


Figure 2. Comparison of some computed inversions with the true inversion of the Equation 21 distribution. Inversions computed from 11 point data sets without added noise. Solid line = true inversion; broken line = computed inversion.

2a. Inversion computed by Spline.



2b. Inversion computed by BARR.



2c. Inversion computed by C & B 3.

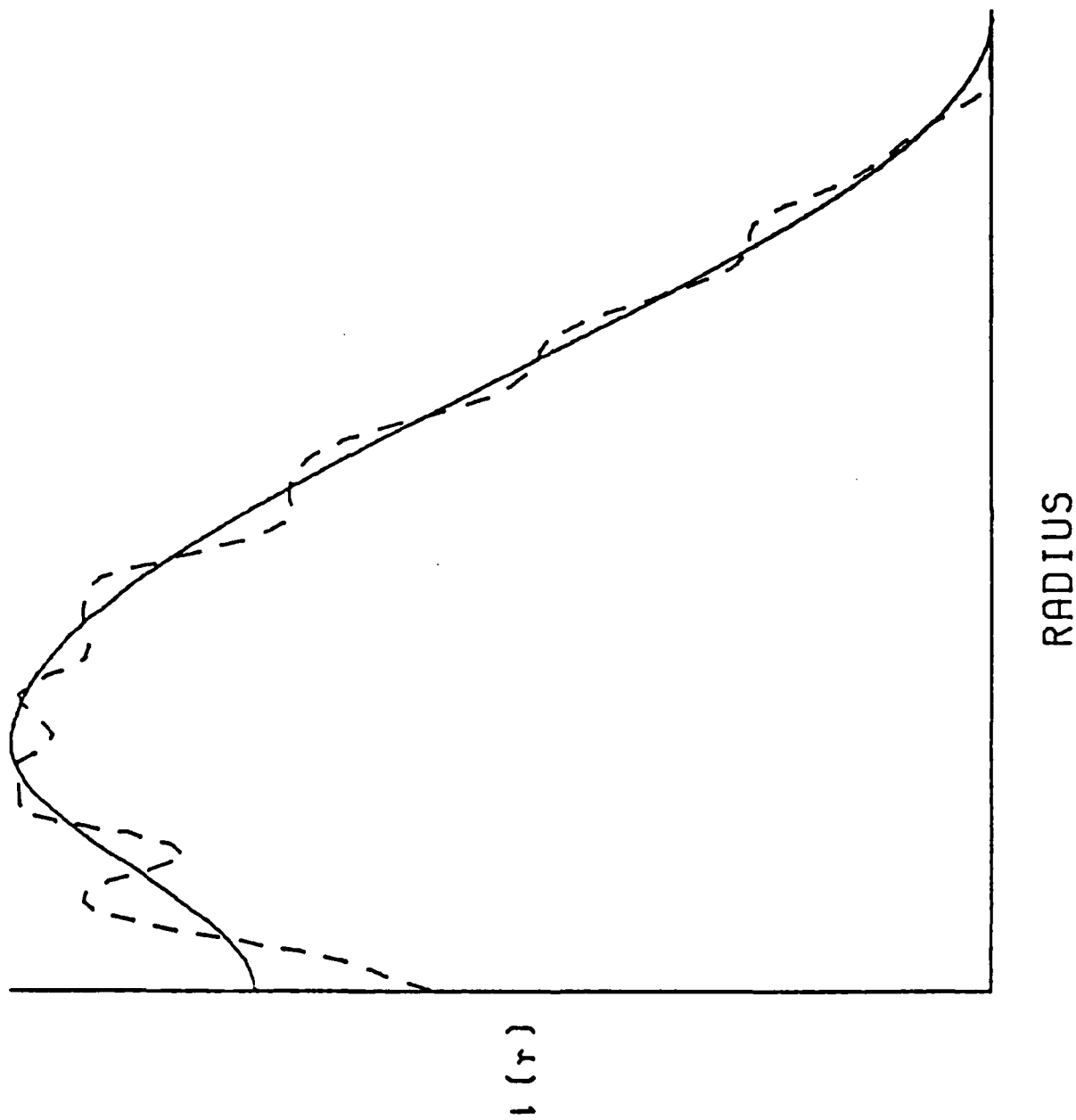
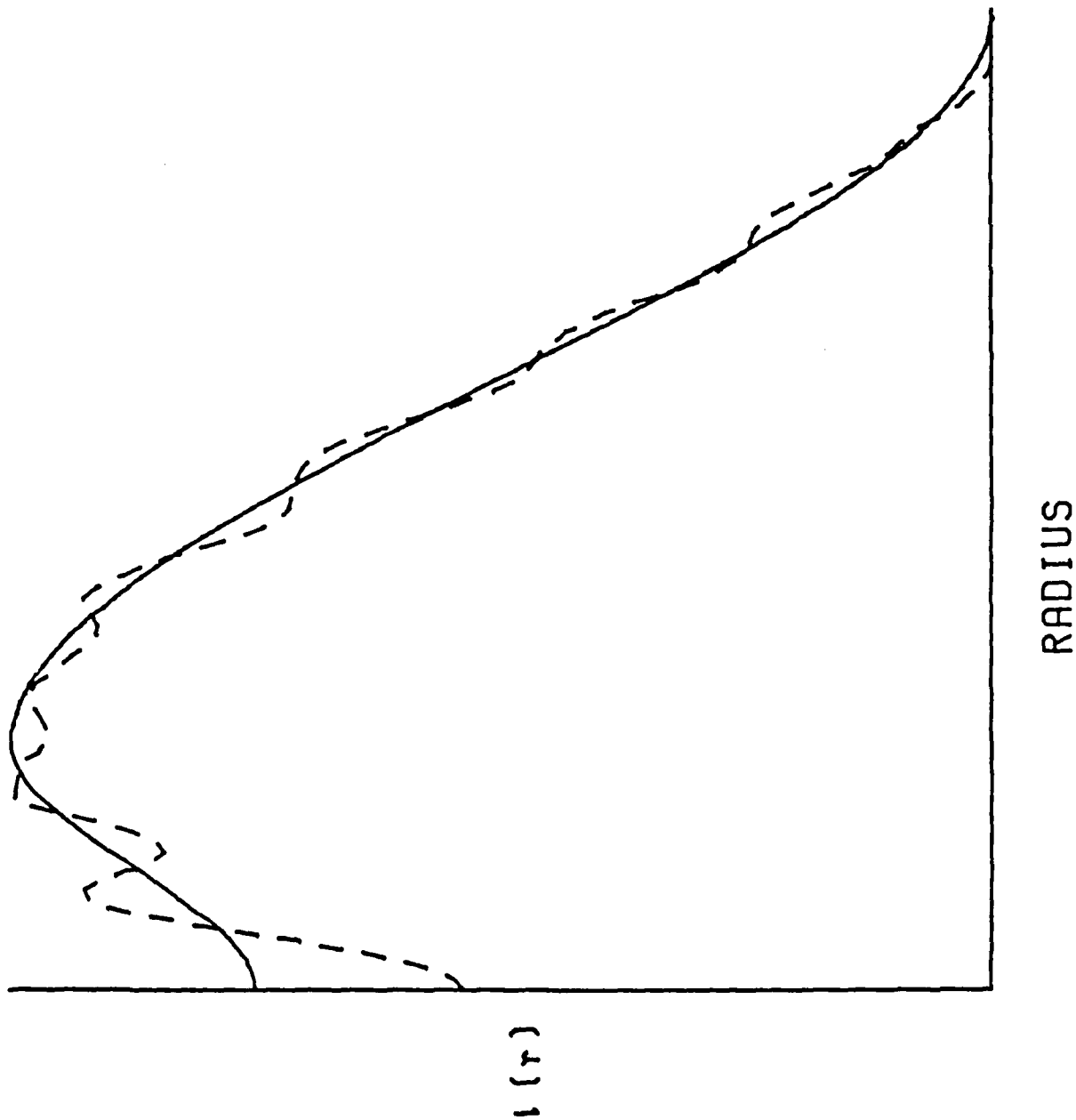


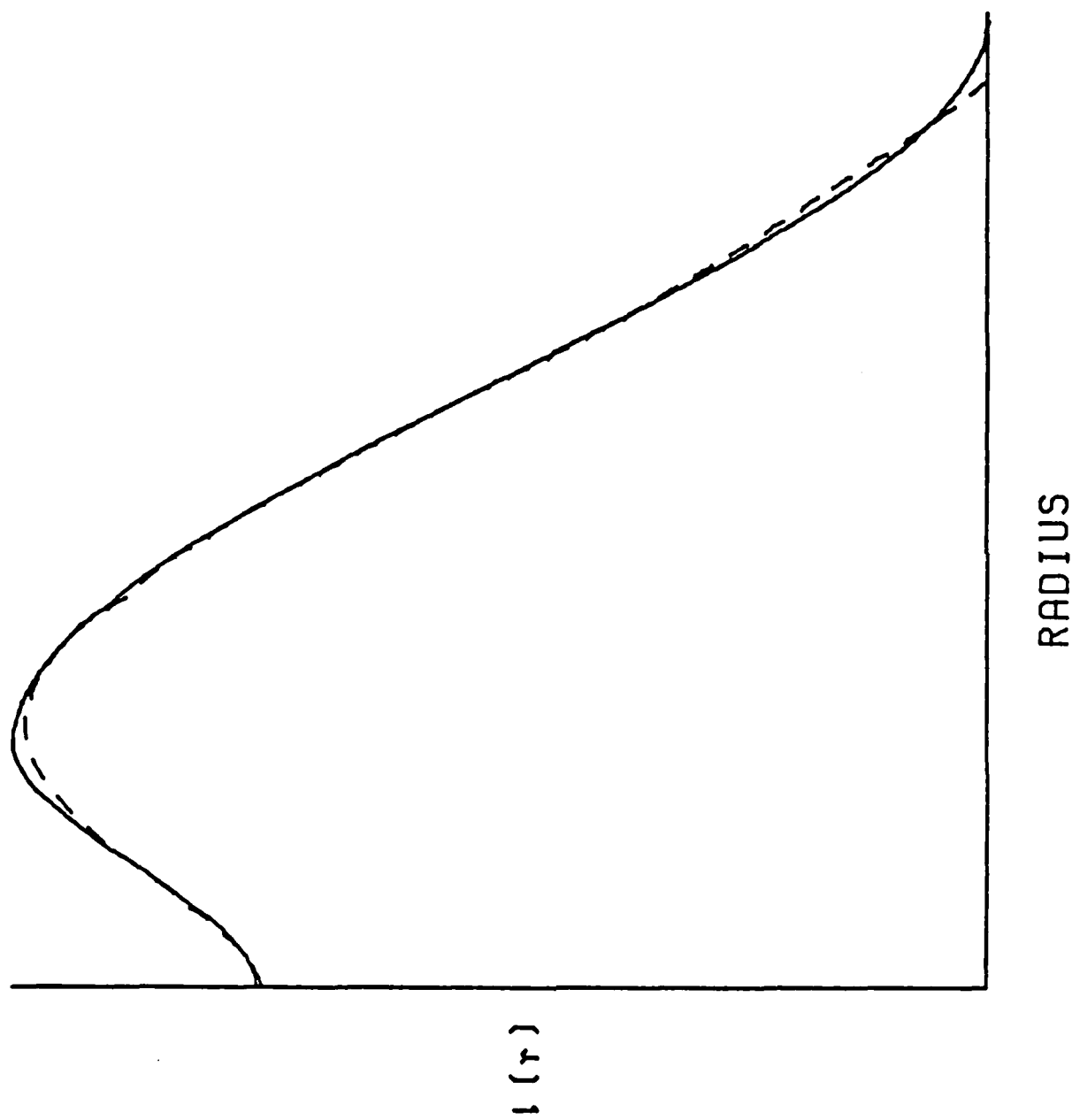
Figure 3. Comparison of some computed inversions with the true inversion of the Equation 21 distribution. Inversions computed from 51 point data sets having 5% noise added. Solid line = true inversion; broken line = computed inversion.

3a. Inversion computed by SPLINE.



3b. Inversion computed by BARR.





3c. Inversion computed by C & B 3.

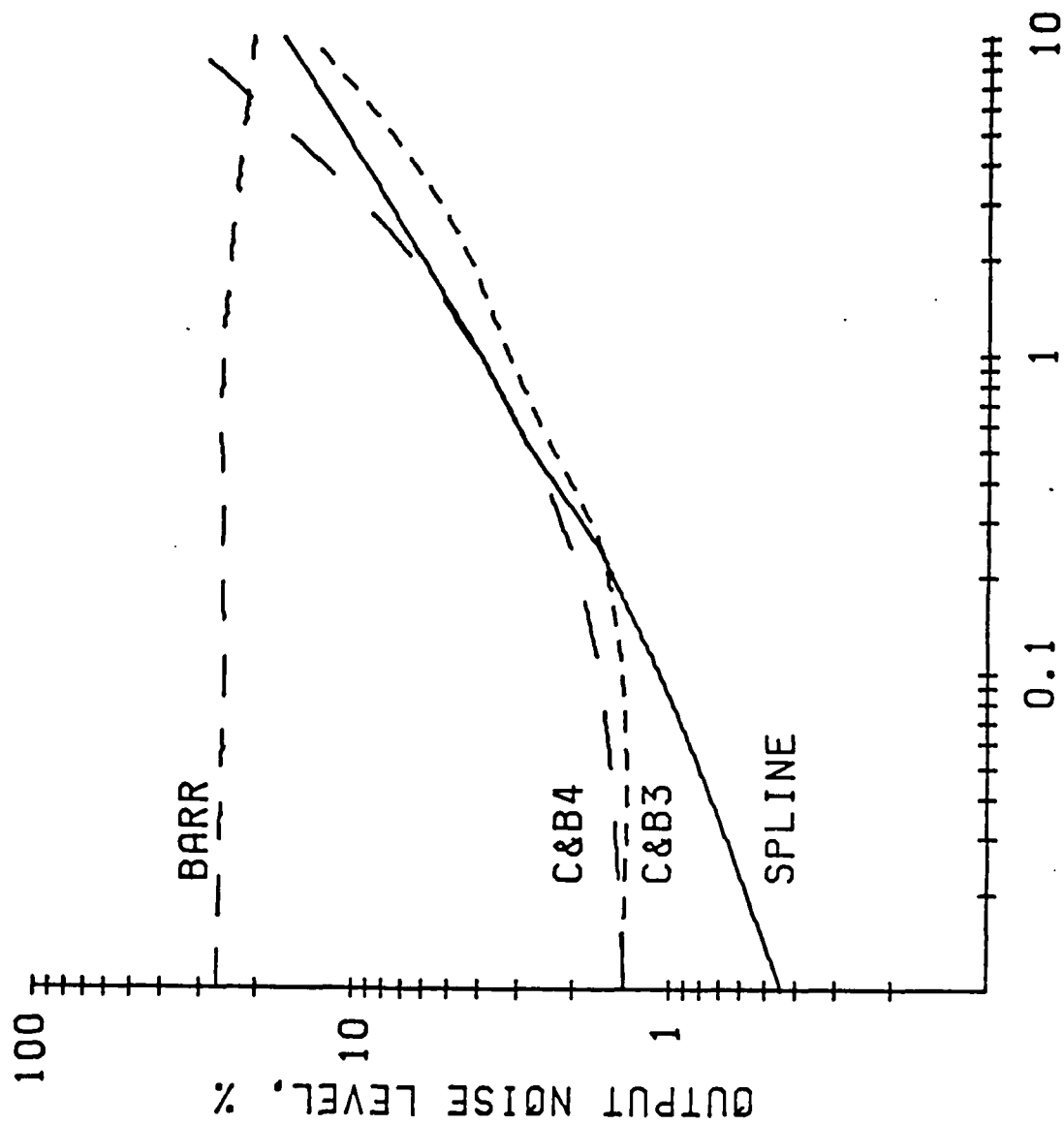


Figure 4. Noise level in the computed inversion as a function of the noise level in the input data for 11 point data sets from Equation 21.

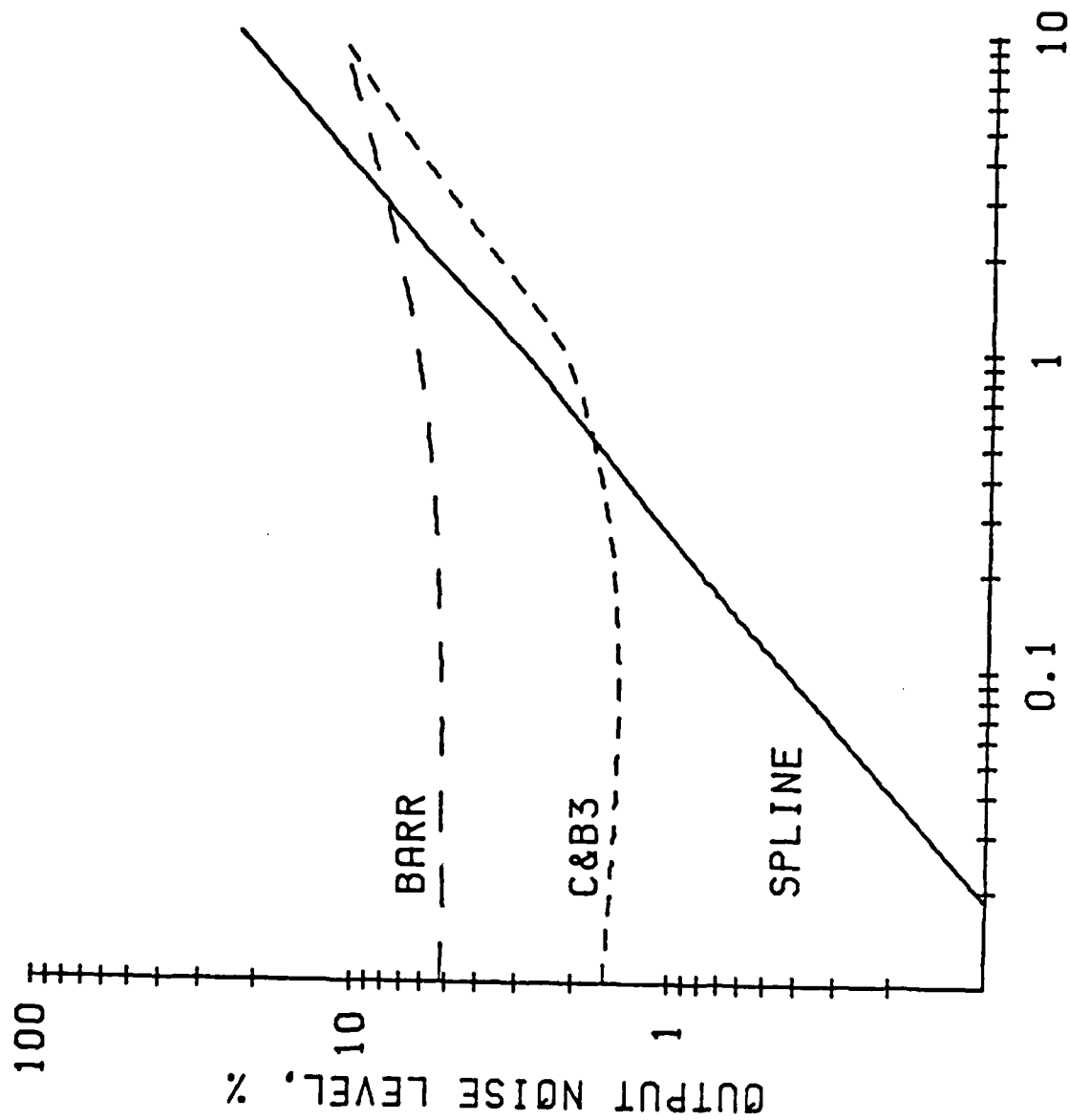


Figure 5. Noise in the computed inversion as a function of the noise level in the input data for 21 point data sets from Equation 21.

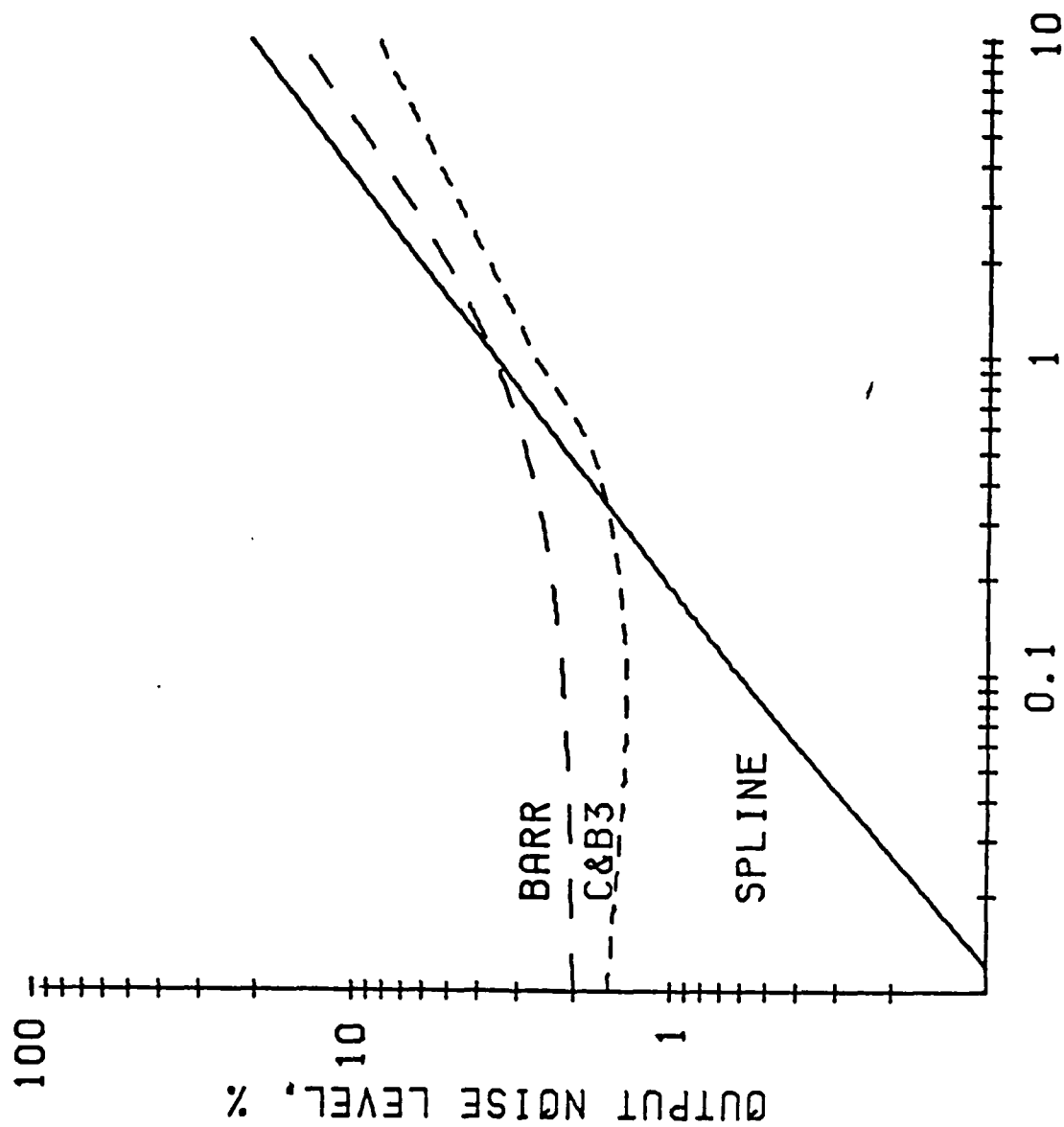


Figure 6. Noise in the computed inversion as a function of the noise level in the input data for 31 point data sets from Equation 21.

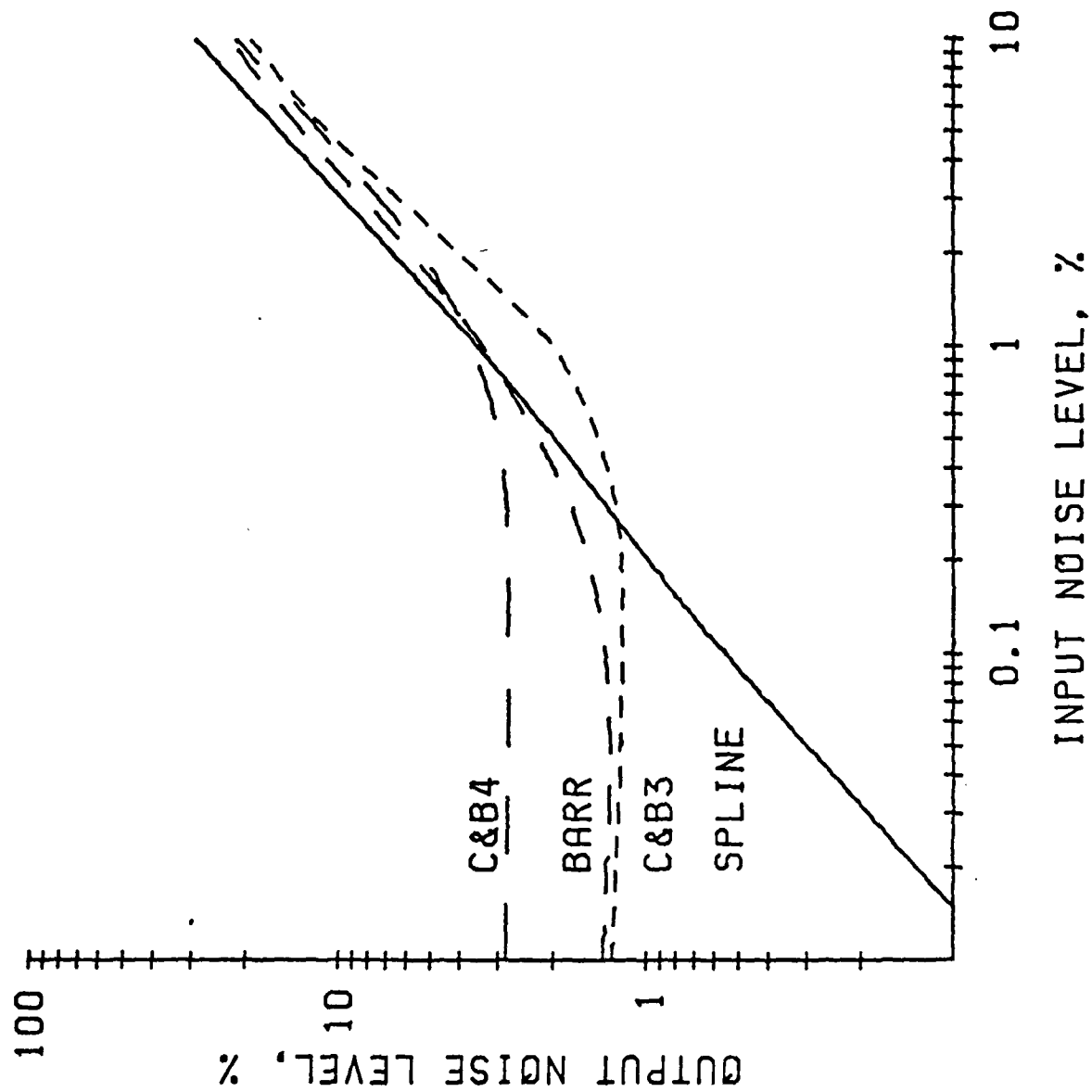


Figure 7. Noise in the computed inversion as a function of the noise level in the input data for 41 point data sets from Equation 21.

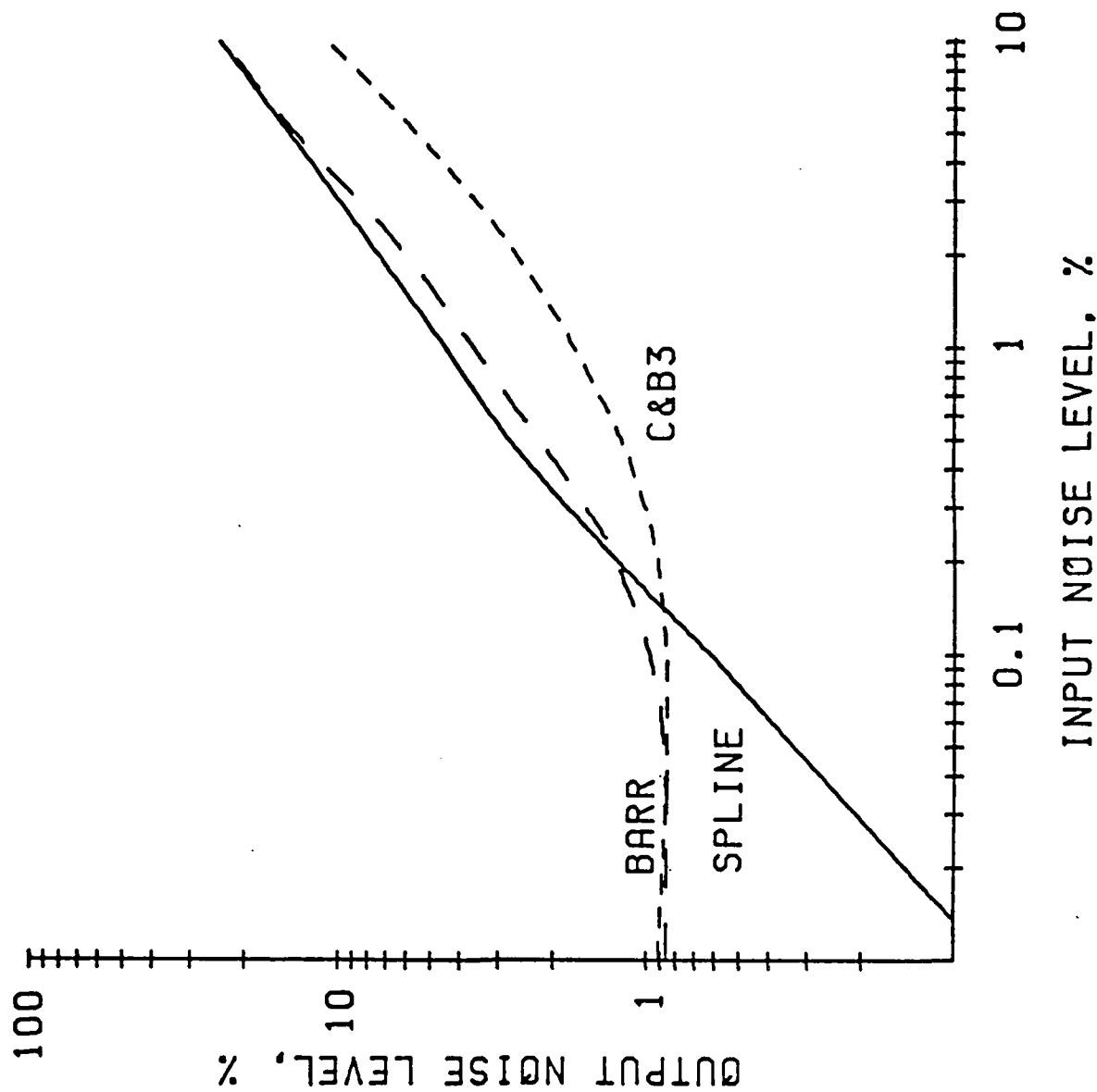


Figure 8. Noise in the computed inversion as a function of the noise level in the input data for 51 point data sets from Equation 21.

# Appendix - Computation of $\beta_{kn}$

The table of coefficients,  $\beta_{kn}$ , used in the Barr method may be computed for a system having  $N + 1$  points by the following algorithm (22).

The table is general, and may be used for any smaller data set.

Copies of the table for  $N=51$  are available from the authors.

For  $k: = 0$ , step 1 until  $N$

do begin

$$K_k = 4430k^6 - 704k^4 + 3352k^2 + 57.6$$

$$C_0 = (-448k^5 - 1088k^4 + 96k^3 + 819.2k^2 + 426.4k - 2.4)/K_k$$

$$C_1 = (-224k^5 + 544k^4 - 1920k^3 - 212.8k^2 - 158.8k + 38.4)/K_k$$

$$C_2 = (1088k^4 - 1212.8k^2 - 72)/K_k$$

$$C_3 = (224k^5 + 544k^4 + 1920k^3 - 212.8k^2 + 158.8k + 38.4)/K_k$$

$$C_4 = (448k^5 - 1088k^4 - 96k^3 + 819.2k^2 - 426.4k - 2.4)/K_k$$

For  $n: = 0$ , step 1 until  $N$

do begin

IF  $k < 2$  or  $n - k \geq 2$

$$\beta_{kn} = \sum_{i=0}^4 C_i \alpha_{kn}$$

ELSE IF  $n - k \geq -2$

$$\beta_{kn} = \sum_{i=0}^{n-k+2} C_i \alpha_{k-2+i,n}$$

end

end

TECHNICAL REPORT DISTRIBUTION LIST, GEN

	<u>No.</u> <u>Copies</u>		<u>No.</u> <u>Copies</u>
Office of Naval Research Attn: Code 472 800 North Quincy Street Arlington, Virginia 22217	2	U.S. Army Research Office Attn: CRD-AA-IP P.O. Box 1211 Research Triangle Park, N.C. 27709	1
ONR Branch Office Attn: Dr. George Sandoz 536 S. Clark Street Chicago, Illinois 60605	1	Naval Ocean Systems Center Attn: Mr. Joe McCartney San Diego, California 92152	1
ONR Area Office Attn: Scientific Dept. 715 Broadway New York, New York 10003	1	Naval Weapons Center Attn: Dr. A. B. Amster, Chemistry Division China Lake, California 93555	1
ONR Western Regional Office 1030 East Green Street Pasadena, California 91106	1	Naval Civil Engineering Laboratory Attn: Dr. R. W. Drisko Port Hueneme, California 93401	1
ONR Eastern/Central Regional Office Attn: Dr. L. H. Peebles Building 114, Section D 666 Summer Street Boston, Massachusetts 02210	1	Department of Physics & Chemistry Naval Postgraduate School Monterey, California 93940	1
Director, Naval Research Laboratory Attn: Code 6100 Washington, D.C. 20390	1	Dr. A. L. Slafkosky Scientific Advisor Commandant of the Marine Corps (Code RD-1) Washington, D.C. 20380	1
The Assistant Secretary of the Navy (RE&S) Department of the Navy Room 4E736, Pentagon Washington, D.C. 20350	1	Office of Naval Research Attn: Dr. Richard S. Miller 800 N. Quincy Street Arlington, Virginia 22217	1
Commander, Naval Air Systems Command Attn: Code 310C (H. Rosenwasser) Department of the Navy Washington, D.C. 20360	1	Naval Ship Research and Development Center Attn: Dr. G. Bosmajian, Applied Chemistry Division Annapolis, Maryland 21401	1
Defense Technical Information Center Building 5, Cameron Station Alexandria, Virginia 22314	12	Naval Ocean Systems Center Attn: Dr. S. Yamamoto, Marine Sciences Division San Diego, California 91232	1
Dr. Fred Saalfeld Chemistry Division, Code 6100 Naval Research Laboratory Washington, D.C. 20375	1	Mr. John Boyle Materials Branch Naval Ship Engineering Center Philadelphia, Pennsylvania 19112	1



TECHNICAL REPORT DISTRIBUTION LIST, 051C

	<u>No. Copies</u>		<u>No. Copies</u>
<del>Dr. M. B. Denton</del> <del>Department of Chemistry</del> <del>University of Arizona</del> <del>Tucson, Arizona 85721</del>	<del>1</del>	Dr. John Duffin United States Naval Postgraduate School Monterey, California 93940	1
Dr. R. A. Osteryoung Department of Chemistry State University of New York at Buffalo Buffalo, New York 14214	1	Dr. G. M. Hieftje Department of Chemistry Indiana University Bloomington, Indiana 47401	1
Dr. B. R. Kowalski Department of Chemistry University of Washington Seattle, Washington 98105	1	Dr. Victor L. Rehn Naval Weapons Center Code 3813 China Lake, California 93555	1
Dr. S. P. Perone Department of Chemistry Purdue University Lafayette, Indiana 47907	1	Dr. Christie G. Enke Michigan State University Department of Chemistry East Lansing, Michigan 48824	1
Dr. D. L. Venezky Naval Research Laboratory Code 6130 Washington, D.C. 20375	1	Dr. Kent Eisentraut, MBT Air Force Materials Laboratory Wright-Patterson AFB, Ohio 45433	1
Dr. H. Freiser Department of Chemistry University of Arizona Tucson, Arizona 85721		Walter G. Cox, Code 3632 Naval Underwater Systems Center Building 148 Newport, Rhode Island 02840	1
Dr. Fred Saalfeld Naval Research Laboratory Code 6110 Washington, D.C. 20375	1	Professor Isiah M. Warner Texas A&M University Department of Chemistry College Station, Texas 77840	1
Dr. H. Chernoff Department of Mathematics Massachusetts Institute of Technology Cambridge, Massachusetts 02139	1	Professor George H. Morrison Cornell University Department of Chemistry Ithaca, New York 14853	1
Dr. K. Wilson Department of Chemistry University of California, San Diego La Jolla, California	1	Dr. Rudolph J. Marcus Office of Naval Research Scientific Liaison Group American Embassy APO San Francisco 96503	1
Dr. A. Zirino Naval Undersea Center San Diego, California 92132	1	Mr. James Kelley DTNSRDC Code 2803 Annapolis, Maryland 21402	1